Л.Н. Гумилев атындағы Еуразия ұлттық университетінің ХАБАРШЫСЫ.
ISSN: 2616-7263. eISSN: 2663-1261
ТЕХНИКАЛЫҚ ҒЫЛЫМДАР ЖӘНЕ ТЕХНОЛОГИЯЛАР СЕРИЯСЫ /
TECHNICAL SCIENCES AND TECHNOLOGY SERIES/
СЕРИЯ ТЕХНИЧЕСКИЕ НАУКИ И ТЕХНОЛОГИИ

IRSTI 67.01.00
Article

https://doi.org/10.32523/2616-7263-2025-152-3-9-22

Evaluating the Seismic Response of CFS Strap-Braced Walls with Optimised Sections

Muhammed Cosut

School of Mechanical, Aerospace and Civil Engineering, The University of Sheffield, Sheffield, UK

E mail: mcosut1@sheffield.ac.uk

Abstract. Cold-formed steel (CFS) profiles are widely used in light steel-framed buildings, particularly for low- to mid-rise construction, where CFS strap-braced frames serve as key lateral load-resisting systems. This research focuses on the seismic performance of strap-braced walls incorporating CFS members, with a particular emphasis on optimising stud elements to function efficiently as beam-columns. A typical cross-section, derived from commercially available profiles, is selected and refined to maximise structural capacity while adhering to industry standards and practical limitations. Finite element (FE) models are developed for two strap-braced wall frames, where the sections are used for both the studs and chords: one frame uses commercially available CFS sections, while the other employs optimised sections aimed at enhancing seismic performance. While conventional designs include gravity loads, they often overlook P-Δ effects; this study addresses that limitation by applying different axial compression levels to assess the impact of P-Δ effects on both developed models. The structural performance is evaluated based on lateral drift compliance and the avoidance of premature failure caused by P-Δ effects in the chord studs. The outcomes offer valuable insights for enhancing the seismic design of CFS structures, presenting a systematic optimisation strategy that improves ductility, reliability, and structural integrity under seismic loading.

Keywords: Cold-Formed Steel; Strap-braced wall panels; Optimization, Gravity loading, Seismic performance

Received 30.08.2025. Revised 05.09.2025. Accepted 08.09.2025. Available online 30.09.2025

*the corresponding author

Introduction

CFS is widely valued in construction due to its excellent strength-to-weight ratio, long-lasting durability, and recyclability, qualities that contribute to its sustainability and cost-effectiveness [1-2]. Its lightweight characteristics enable easier transportation and faster installation. Additionally, CFS's adaptability allows for efficient section design and off-site manufacturing, which reduces material waste and shortens construction durations. In multi-storey buildings, CFS members frequently act as the primary lateral force-resisting elements, effectively supporting both vertical and lateral loads from wind and seismic forces [3-7]. In these systems, lateral load resistance is commonly provided by strap-braced stud walls [8-10], which are available in various forms such as X-bracing [11], K-bracing [12], knee-bracing, or combinations thereof.

Several researchers have investigated the behaviour of CFS strap-braced walls, particularly under monotonic and cyclic loading conditions. Al-Kharat and Rogers [11] performed experimental tests on light, medium, and heavy CFS strap-braced walls and found that heavier panels showed inadequate ductility. Likewise, Zeynalin and Ronagh [13] examined strap-braced walls with a 1:1 aspect ratio, focusing on the effects of strap quantity, angles, and bracket design under cyclic loads. Their results indicated that these walls maintained stable hysteretic behaviour and could be considered structurally dependable. Although shake-table tests conducted by others [14] have contributed valuable insights into CFS wall behaviour, the combined impact of gravity and lateral loads has often been neglected. Rad et al. [15] addressed this gap by performing full-scale cyclic tests on two-story CFS strap-braced systems, demonstrating robust elastic-plastic responses when appropriate detailing was implemented.

Optimization methods are commonly applied in structural engineering to enhance load capacity and stiffness or to reduce cost, weight, and carbon emissions. Depending on the design goals, various algorithms (such as metaheuristic, deterministic gradient-based, or hybrid approaches) can be employed. For example, Ye et al. [16-187] increased the load-carrying capacity of beams by optimizing cross-sectional designs incorporating edge and intermediate stiffeners and segmented folded flanges. Similarly, Mojtabaei et al. [19-20] developed a metaheuristic-based methodology to optimize CFS beam-column members, maximizing their load capacity while maintaining consistent material usage in compliance with Eurocode 3.

This study focuses on improving the load-bearing capacity of CFS strap-braced walls by substituting the commercially available stud and chord sections with optimized alternatives. The optimization process was constrained by material usage limits, specifically the total coil width and thickness of the chosen sections. FE models of walls with both commercially available and optimized stud sections were created and analysed under combined gravity and lateral loading to assess seismic performance. The subsequent sections of this paper include Section 2, which details the design process for the CFS beam-column elements; Section 3, which describes the optimization methodology and associated constraints; Section 4, covering the development and validation of the FE model; and Section 5, which presents the seismic performance evaluation.

The methodology

CFS beam-column element design

The design of CFS elements has been extensively investigated in previous studies using both prescriptive code-based methods and data-driven approaches [21-23]. In this study, the capacity

of the CFS beam-column element was determined using the EN1993-1-1 [24] and EN1993-1-3 [25] standards. The cross-sectional resistance was evaluated by considering both local and distortional buckling modes, while the member resistance accounted for global instabilities.

Local-distortional buckling and cross-section check

The Effective Width Method (EWM) outlined in Eurocode 3 addresses local buckling by reducing the load-bearing capacity of compressed plate regions. This reduction may cause a shift in the centroid position and result in additional bending moments. When the member is subjected to bending, an iterative procedure is employed to determine the neutral axis and compute the bending strength based on the effective partially plastic section modulus. Distortional buckling, which frequently occurs in stiffened plates under flexural or flexural-torsional loads, involves both in-plane and out-of-plane deformation modes. Eurocode 3 manages this phenomenon by decreasing the effective thickness of the stiffener and the adjacent plate areas. The buckling stress is then calculated by modelling the stiffened section as a compression element resting on an elastic foundation.

The cross-section of a CFS beam-column under axial compression and bending moments must satisfy the following criteria:

$$\frac{N_{Ed}}{N_{c,Rd}} + \frac{M_{y,Ed} + \Delta M_{y,Ed}}{M_{cy,Rd}} + \frac{M_{z,Ed} + \Delta M_{z,Ed}}{M_{cz,Rd}} \leq 1 \quad (1)$$

where $N_{c,Rd}$ denotes the design compressive resistance of the cross-section, while $M_{cy,Rd}$ and $M_{cz,Rd}$ design moment resistance about the major (y-axis) and the minor (z-axis) axes, respectively. The additional moments are calculated as $\Delta M_{y,Ed} = N_{Ed} e_{Ny}$ and $\Delta M_{z,Ed} = N_{Ed} e_{Nz}$, where e_{Ny} and e_{Nz} are the shifts of the y- and z-axes, respectively.

Member resistance requires various calculations for both pure compression and pure bending. In this regard, global buckling is considered for pure compression, while lateral-torsional buckling is assessed under pure bending. Additionally, member stability was evaluated using the equations provided in EN 1993-1-3.

The optimization in this study utilized the code developed by Mojtabaei et al. [19], which is based on the Particle Swarm Optimization (PSO) technique. The primary goal was to keep the material consumption, specifically the total coil width, consistent with that of the commercially available reference section used as a baseline. Using this reference, an optimized cross-sectional design was created to improve the load capacity under combined axial compression (N_{Ed}) and bending about the major axis ($M_{y,Ed}$). The bending moment was applied by introducing an eccentricity (e_y) to the axial compressive load, thereby maximizing the axial capacity N_{Ed} under conditions that closely simulate real-world loading ($M_{y,Ed} = N_{Ed} \times e_y$).

During the optimization, a beam-column element with simply supported end-fork supports was modelled, which permitted rotations and warping at its ends but restricted twisting along the longitudinal axis. The study focused on a lipped channel section and explored various parameters, such as section thicknesses of 1.16, 2, 3, and 4 mm, as well as eccentricities of 0, 100, and 300 mm. These variations were analysed to assess and compare the enhancements in axial compressive load capacity for each scenario. To maximize the axial load capacity, the cross-sectional optimization combined the Eurocode Design Procedure for Beam-Column Members with a Particle Swarm Optimization tool implemented in MATLAB.

Figure 1 illustrates both the original and optimized cross-sectional designs. Furthermore, Table 1 outlines the specific restrictions and requirements imposed by industry standards and

manufacturing processes. The design variables primarily involved the lengths of the flange and lip, which were limited according to these standards and production considerations. The angle θ was set to π/2. Additional constraints were introduced to accommodate the installation of hold-down devices (Simpson S/HD10 S with a depth of 59 mm) on the CFS strap-braced wall. These constraints ensured that the spacing between the lips of the chord members provided sufficient clearance for the hold-downs to be properly installed without causing any interference with the chord cross-sectional shape, as detailed below:

$$spacing \geq h - 2 \times c = 60 \quad (2)$$

where h denotes the web height and c represents the lip length.

Table 1. Optimization design variables, constraints and limitations

Design variables	Constraints based on EC3	Manufacturing & practical limitations (mm)
$\boldsymbol{X_1 = c/b}$ $\boldsymbol{X_2 = b/L}$	$0.2 \leq c/b \leq 0.6$ $b/t \leq 60$ $c/t \leq 50$ $h/t \leq 500$ $\pi/4 \leq \theta \leq 3\pi/4$	$b \geq 30$ $c \geq 10$ $h \geq 2csin(\theta)$

Design variables which are X_1 and X_2 ratio ranges were computed based on the standard and manufacturing process. X_1 was set between 0.2 and 0.6, while X_2 was determined based on the total coil width and material thickness. The maximum ratio for X_2 was limited using two different arrangements to reduce the computational time by narrowing the range.

$$\frac{b_{min}}{L} \leq X_2 \leq \min \begin{cases} \dfrac{60 \times t}{L} \\ \dfrac{b_{msx}}{L} \end{cases} \quad (3)$$

$$b_{msx} = L - h_{min} - 2 \times c_{min} \quad (4)$$

where b_{min} was set 30 mm, L is the total coil width (300 mm), t, h_{min}, c_{min} represent the thickness, minimum web height and minimum lip length, respectively.

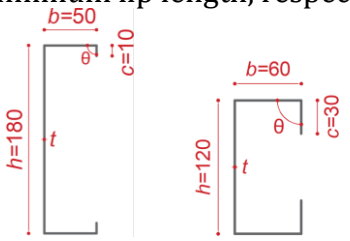

(a) (b)

Figure 1 Cross-section of (a) commercially available, (b) optimised section

Particle Swarm Optimization (PSO)

Particle Swarm Optimization (PSO) is a metaheuristic technique rooted in the collective behavior observed in nature among groups like birds, fish, and ants. This method belongs to the broader family of swarm intelligence algorithms. In PSO, each particle adjusts its velocity by considering both its personal best experience and the best performance achieved by the swarm as a whole. This approach enables a balanced integration of individual adaptation and collaborative decision-making, making the algorithm highly effective for solving complex optimization problems. FE modelling: descriptions and properties.

Abaqus [26] is well-established for its effectiveness in precisely replicating the structural response of CFS structures, significantly reducing the reliance on large-scale physical testing [27-30]. Following the optimization of the C-lipped section with zero eccentricity (e= 0), FE models of CFS strap-braced walls were developed using both commercially available and optimised stud sections. Each wall model measured 2.44 m × 2.44 m and included top and bottom rigid plates, tracks, chords, studs, X-shaped straps, bridging members, hold-downs, L-brackets, and anchor rods (see Figure 2).

Element type and material characterization

The cold-formed steel (CFS) strap-braced wall models were developed using four-node S4R shell elements, which are well-suited for analysing thin-walled components. To ensure accuracy and efficiency, a mesh sensitivity study was conducted, resulting in a mesh size of 15 mm × 15 mm for most structural elements, while rigid plates were assigned a coarser mesh of 20 mm × 20 mm to optimize computational performance. Material properties were obtained from experimental tests, and stress-strain data were converted to true stress-strain relationships for accurate Abaqus input. The elastic modulus is 203 GPa, and the Poisson's ratio is 0.3. Strap and track have the same yield (f_y) and ultimate stress (f_u) as 296 and 366 MPa, respectively. Also, stud and chord have the same f_y and f_u of 325 and 382 MPa, respectively. In addition, the isotropic hardening model was used for the monotonic analysis.

Table 2*:* Material properties

	f_y (MPa)	f_u (MPa)
Strap Track	296	366
Stud Chord	325	382

Boundary conditions, loading, and connection modelling

In the FE model, the hold-downs (Simpson S/HD10 S) and tracks were connected to reference points positioned at the anchor locations. These reference points at the base were fully fixed, while those at the top were permitted to move laterally within the plane. However, their out-of-plane translations and rotational degrees of freedom were restrained. A monotonic load was applied incrementally until the inter-storey drift reached a maximum limit of 5%. To replicate gravity loading, a 20 mm thick plate was added above the top track, facilitating even distribution of vertical loads. This top plate was subjected to uniform pressure, scaled based on the compressive capacities of the vertical members, as outlined in EN1993-1-3 [25]. The connections between tracks and studs, as well as straps and chords, were simulated using empirical formulations proposed by Pham and Moen [31]. Within Abaqus [26], screws were modelled as discrete fasteners, with the connector influence radius enabling the transfer of displacements and rotations from surface nodes to the fastening locations.

Geometric Imperfection

Initial geometric imperfections were incorporated by scaling the first buckling mode shape from an eigenvalue buckling analysis [32-35]. Slack in tension straps was simulated by applying unit lateral displacements at anchor points, inducing initial compression in the diagonals. Chord stud imperfections were omitted due to their negligible impact, enhancing computational

efficiency in multi-storey models.

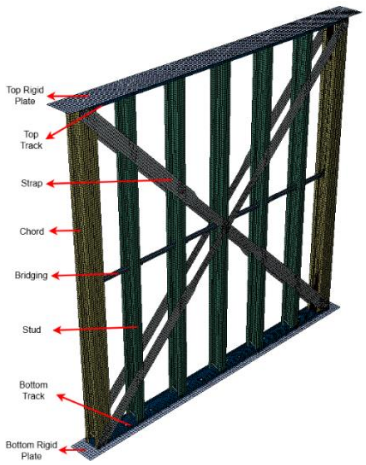

Figure 2. FE model

Findings/Discussion

In the optimization process, three different values of e (0, 100, and 300) were considered, along with four thicknesses (1.16, 2, 3, and 4) for the C-lipped stud element. These combinations were analysed to explore the relationship between e and thickness. The results show that as e increases, the capacity improvements between commercially available and optimised sections become smaller. To exemplify, the capacity improvement for e=0 ranges from approximately 42% to 91%, while for e=300, it ranges from about 8% to 25% (see Figure 3). Consequently, the differences in average capacity improvement of approximately 45% and 12% can be observed between e=0 and e=300, as well as between e=100 and e=300, respectively.

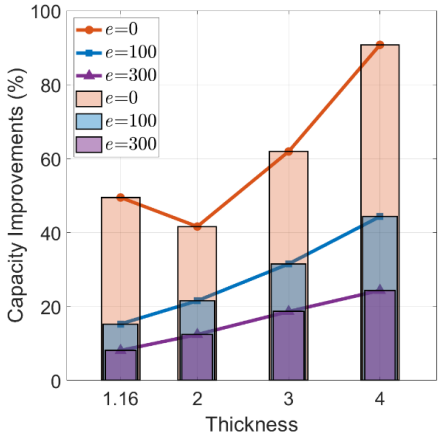

Figure 3 Optimization results based on thickness

Once the CFS strap-braced wall frames using both commercially available and optimised stud sections were created in Abaqus, the gravity load, calculated based on commercially available sections considering the total compressive strength of the vertical elements ($N_{b,t}$), was applied to

both frames across a range of load levels. This was done to examine the P- Δ responses of the models and to assess whether they reached the maximum allowable drift. Figure 4 illustrates the FE analysis results, showing the effects of applying gravity loads ranging from 0% to 50% $N_{b,t}$ on both frames. The analysis was conducted using 2 mm thick straps and 1.16 mm thick chords, and studs. The CFS strap-braced frame equipped with the optimised section (see Figure 4 (b)) demonstrated consistent performance, with most frames achieving the maximum allowable drift. However, the frames subjected to 43% and 50% $N_{b,t}$ are unable to reach this limit. In contrast, the CFS strap-braced frame equipped with a commercially available stud section (see Figure 4 (a)) showed a noticeable reduction in performance, failing to reach the maximum allowable drift at several load levels between 22% and 50% $N_{b,t}$.

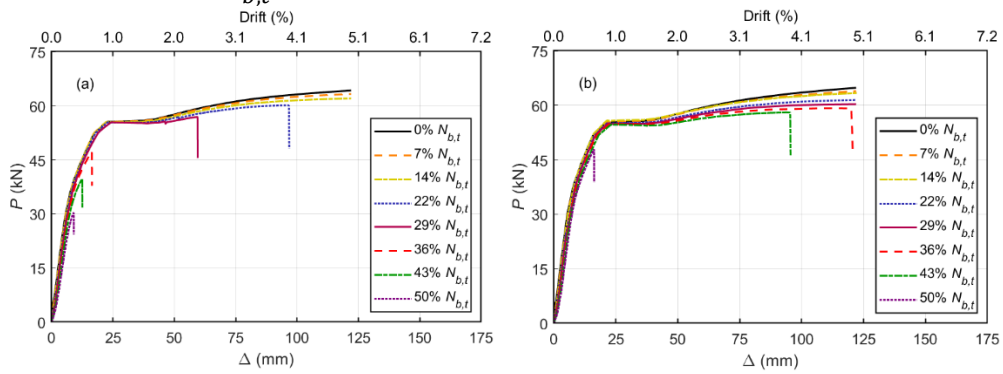

Figure 4 Monotonic response of (a): commercially available; (b): optimised models

The stiffness (k) (kN/mm) and ductility (μ) values were computed using the bilinear curve, which follows the Equivalent Energy Elastic-Plastic (EEEP) approach [36]. These values are determined as follows:

$$k = \frac{P_y}{\Delta_y} \tag{5}$$

$$\mu = \frac{\Delta_u}{\Delta_y} \tag{6}$$

where P_y is the yield load, Δ_y is the yield displacement, and Δ_u is the ultimate displacement.

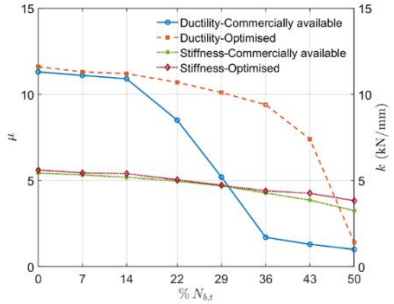

Figure 5 Evaluation of ductility ratio (μ) and stiffness (k) of the commercially available and optimised section under varying $N_{b,t}$

Based on monotonic analysis results, the stiffness and ductility of both CFS strap-braced frames, equipped with commercially available and optimised stud sections, were evaluated under varying vertical load ratios (% $N_{b,t}$) (see Figure 5). The stiffness of both models exhibits a similar

decreasing trend, with a gradual reduction as the vertical load increases. For frames with commercially available stud sections, ductility shows a slight decline from 0% to 14% $N_{b,t}$, followed by a significant drop beyond this point. In contrast, frames with optimised stud section maintains higher ductility up to 36% $N_{b,t}$, with a noticeable reduction occurring only at higher vertical load levels. A sharp drop is observed particularly at 50% N_(b,t), where the ductility value reaches approximately 1.4.

Conclusion

This study aimed to enhance the performance of CFS strap-braced frames by optimising stud (beam–column) sections within design and manufacturing constraints. The optimised cross-section was applied to both studs and chords, and FE models were developed in Abaqus using both commercially available and optimised stud sections. Combined gravity and lateral loads were applied to the frames, with the total gravity load calculated based on the compressive strength of the vertical elements (i.e., chords and studs) in the commercially available section. This reference value was then used to define gravity load levels ranging from 0% to 50% of $N_{b,t}$, and consistently applied to both frames. This approach enabled a consistent comparison of stiffness, strength, and ductility across configurations. The findings demonstrate that variations in eccentricity (e) and thickness during beam–column element optimization significantly influence the improvement of the load-bearing capacity, revealing clear differences between the optimised and commercially available sections. Moreover, increased eccentricity results in reduced capacity.

While low vertical loads have a minimal impact on lateral performance, higher gravity loads considerably enhance the peak strength, ductility, and stiffness of frames incorporating the optimised section, in contrast to those using commercially available section.

References

1. M. Hasanali, K. Roy, S.M. Mojtabaei, I Hajirasouliha, GC Clifton, JBP Lim A critical review of cold-formed steel seismic resistant systems: Recent developments, challenges and future directions. Thin-Walled Structures 180, (2022) 109953.
2. D.T. Phan, S.M. Mojtabaei, I. Hajirasouliha, J. Ye, J.B.P Lim. Coupled Element and Structural Level Optimisation Framework for Cold-Formed Steel Frames, Journal of Constructional Steel Research, 49 (2019) 69-83.
3. Papargyriou, S.M. Mojtabaei, I. Hajirasouliha, J. Becque, K. Pilakoutas, Cold-formed steel beam-to- column bolted connections for seismic applications, Thin-Walled Structures, 172 (2022) 108876.
4. J. Ye, S.M. Mojtabaei, I. Hajirasouliha, K. Pilakoutas, Efficient design of cold-formed steel bolted-moment connections for earthquake resistant frames, Thin-Walled Structures, 59 (2019) 49-61.
5. J. Ye, S.M. Mojtabaei, I. Hajirasouliha. Seismic performance of cold-formed steel bolted moment connections with bolting friction-slip mechanism, Journal of Constructional Steel Research, 27 (2019) 86- 100.
6. S.M. Mojtabaei, I. Hajirasouliha, J. Ye, Optimisation of cold-formed steel beams for best seismic performance in bolted moment connections, Journal of Constructional Steel

Research, 181 (2021) 106621.
7. S.M. Mojtabaei, M.Z. Kabir, I. Hajirasouliha, M. Kargar, Analytical and experimental study on the seismic performance of cold-formed steel frames. Journal of Constructional Steel Research 143, (2018) 18-31.
8. . Yilmaz, S.M. Mojtabaei, I. Hajirasouliha, J. Becque, Behaviour and performance of OSB-sheathed cold- formed steel stud wall panels under combined vertical and seismic loading, Thin-Walled Structures, 183 (2023) 110419.
9. F. Yilmaz, J. Becque, S.M. Mojtabaei, I. Hajirasouliha, Capacity and Behavior of Sheathed Cold-Formed Steel Stud Walls under Outward Flexural Loading. Journal of Structural Engineering 151 (1), (2025) 04024192.
10. F. Yilmaz, J. Becque, S.M. Mojtabaei, I. Hajirasouliha, Experimental investigation of the behaviour and capacity of sheathed cold-formed steel stud walls under inward flexural loading. Thin-Walled Structures 192, (2024) 111048.
11. Al-Kharat, M.; Rogers, C.A. (2007) Inelastic performance of cold-formed steel strap braced walls. Journal of Constructional Steel Research 63, 4, p. 460–474.
12. Riahi, H.T. et al. (2020) Seismic collapse assessment of K-shaped bracings in cold-formed steel frames. Structures 27, p. 1803–1817.
13. Zeynalian, M.; Ronagh, H. (2013) Experimental study on seismic performance of strap-braced cold-formed steel shear walls. Advances in Structural Engineering 16, 2, p. 245–257.
14. Gad, E. et al. (1999) Lateral performance of cold-formed steel-framed domestic structures. Engineering Structures 21, 1, p. 83–95.
15. Rad, P.L. et al. (2024) Experimental investigation on seismic performance of cold-formed steel strap-braced stud walls under lateral cyclic and vertical loading. Thin-Walled Structures 194, p. 111312.
16. J. Ye, S.M. Mojtabaei, I. Hajirasouliha. Local-flexural interactive buckling of standard and optimised cold- formed steel columns, Journal of Constructional Steel Research, 144 (2018) 106-118.
17. J. Ye, S.M. Mojtabaei, I. Hajirasouliha, Paul Shepherd, Kypros Pilakoutas, Strength and deflection behaviour of cold-formed steel back-to-back channels. Engineering Structures 177 (2018) 641-654.
18. J. Ye, J. Becque, I. Hajirasouliha, S.M. Mojtabaei, J.B.P. Lim. Development of optimum cold-formed steel sections for maximum energy dissipation in uniaxial bending, Engineering Structures, 161 (2018) 55-67.
19. Mojtabaei, S.M. et al. (2021) Structural size optimization of single and built-up cold-formed steel beam-column members. Journal of Structural Engineering 147, 4, p. 04021030.
20. S.M. Mojtabaei, J. Ye, I. Hajirasouliha. Development of optimum cold-formed steel beams for serviceability and ultimate limit states using Big Bang-Big Crunch optimisation, Engineering Structures, 195 (2019) 172-181.
21. S.M. Mojtabaei, R. Khandan, I. Hajirasouliha, Predicting restraining effects in CFS channels: A machine learning approach, Steel and Composite Structures, An International Journal 51 (4), 441-456.
22. L. Simwanda, P. Gatheeshgar, F.M. Ilunga, B.D. Ikotun, S.M. Mojtabaei, Explainable machine learning models for predicting the ultimate bending capacity of slotted perforated cold-formed steel beams under distortional buckling, Thin-Walled Structures 205, (2024) 112587

23. S.M. Mojtabaei, J. Becque, I. Hajirasouliha, R. Khandan, Predicting the buckling behaviour of thin-walled structural elements using machine learning methods, Thin-Walled Structures, 184 (2023) 110518.
24. CEN (European Committee for Standardization) (2005) Eurocode 3: Design of steel structures – Part 1-1: General rules and rules for buildings. Brussels, Belgium.
25. CEN (European Committee for Standardization) (2005) Eurocode 3: Design of steel structures – Part 1-3: General rules – Supplementary rules for cold-formed members and sheeting. Brussels, Belgium.
26. Dassault Systèmes Simulia (2014) Abaqus 6.14 CAE User Guide.
27. D.T. Phan, S.M. Mojtabaei, I. Hajirasouliha, T. L. Lau, J.B.P Lim. Design and optimisation of cold-formed steel sections in bolted moment connections considering bimoment, Journal of Structural Engineering (ASCE), 146 (2020) 04020153.
28. S.M. Mojtabaei, J. Becque, I. Hajirasouliha. Local buckling in cold-formed steel moment resisting bolted connections: behaviour, capacity and design, Journal of Structural Engineering (ASCE), 146 (2020) 04020167
29. H. Parastesh, S.M. Mojtabaei, H. Taji, I. Hajirasouliha, A. Bagheri Sabbagh, Constrained optimization of anti-symmetric cold-formed steel beam-column sections, Engineering Structures, 228 (2021) 111452.
30. S.M. Mojtabaei, J. Becque, I. Hajirasouliha, Behavior and Design of Cold-Formed Steel Bolted Connections Subjected to Combined Actions, Journal of Structural Engineering, 147 (2021) 04021013.
31. Pham, H.S.; Moen, C.D. (2015) *Stiffness and strength of single shear cold-formed steel screw-fastened connections.* Proceedings of the Annual Stability Conference, p. 1–12.
32. M. Hasanali, S.M. Mojtabaei, I. Hajirasouliha, G.C. Clifton, J.B.P. Lim, More accurate design equations for cold- formed steel members subjected to combined axial compressive load and bending, Thin-Walled Structures, 185 (2023) 110588.
33. M. Hasanali, S.M. Mojtabaei, G.C. Clifton, I. Hajirasouliha, S. Torabian, J.B.P. Lim, Capacity and design of cold- formed steel warping-restrained beam-column elements, Journal of Constructional Steel Research, 190 (2022) 107139.
34. F. Öztürk, S.M. Mojtabaei, M. Şentürk, S. Pul, I. Hajirasouliha, Buckling behaviour of cold-formed steel sigma and lipped channel beam–column members, Thin-Walled Structures, 173 (2022) 108963.
35. M. Hasanali, S.M. Mojtabaei, J.B.P. Lim, G.C. Clifton, I. Hajirasouliha, Optimized interaction equations for more efficient design of CFS channels under combined compression and biaxial bending. Journal of Structural Engineering 150 (8), (2024) 04024088.

Мухаммед Косут

Механикалық, аэроғарыштық және азаматтық инженерия мектебі, Шеффилд университеті, Шеффилд, Ұлыбритания

Оптимизацияланған қималары бар CFS (қалыпта суықтай иілген болат) қиғаш байланыстарымен қабырғалардың сейсмикалық әсерін бағалау

Аңдатпа. Суықтай иілген болат (CFS) профильдері жеңіл болаттан жасалған қаңқалы

ғимараттарда кеңінен қолданылады, әсіресе аз және орта қабатты құрылыстарда, мұнда CFS қиғаш байланыстары бар рамалар көлденең жүктемелерге қарсы негізгі жүйелер болып табылады. Бұл зерттеу CFS элементтері енгізілген қиғаш байланыстары бар қабырғалардың сейсмикалық жұмысын зерттеуге бағытталған, әсіресе тіреуіш элементтерді тиімді түрде баған-сүргіш ретінде жұмыс істету үшін оңтайландыруға баса назар аударылады. Саудада бар профильдер негізінде алынған және нақтыланған типтік қима таңдалып, салалық стандарттар мен практикалық шектеулерді сақтай отырып, көтергіштік қабілетті барынша арттыру көзделген. Қиғаш байланыстары бар екі рамалық жүйе үшін соңғы элементтер әдісі (СЭӘ) бойынша модельдер әзірленді: бір рамда коммерциялық қолжетімді CFS қималары қолданылса, екіншісінде сейсмикалық тұрақтылықты арттыруға бағытталған оңтайландырылған қималар пайдаланылды. Дәстүрлі жобаларда ауырлық күштері ескерілгенімен, көбінесе P-Δ әсерлері назардан тыс қалады; бұл зерттеуде бұл шектеу әртүрлі осьтік қысу деңгейлерін қолданып, P-Δ әсерінің екі модельге ықпалын бағалау арқылы шешілген. Құрылымдық жұмыс қабырға ығысу шегіне сәйкестігіне және хорда тіреуіштеріндегі P-Δ әсерінен болатын мерзімінен бұрынғы істен шығуды болдырмауға негізделіп бағаланды. Нәтижелер CFS құрылымдарының сейсмикалық жобалауын жетілдіруге құнды ұсыныстар береді және пластикалылығын, сенімділігін және сейсмикалық жүктемелер кезіндегі құрылымдық тұтастығын арттыратын жүйелі оңтайландыру стратегиясын ұсынады.

Түйін сөздер: суықтай иілген болат; қиғаш байланысы бар қабырғалық панельдер; оңтайландыру; ауырлық жүктемесі; сейсмикалық тұрақтылық.

Мухаммед Косут

Школа машиностроения, аэрокосмической и гражданской инженерии, Университет Шеффилд, Шеффилд, Великобритания

Оценка сейсмической реакции стен с раскосами из холодногнутых профилей с оптимизированными сечениями

Аннотация. Холодногнутые стальные (CFS) профили широко применяются в каркасных зданиях из легкой стали, особенно в мало- и среднеэтажном строительстве, где рамы с раскосами из CFS служат основными системами восприятия горизонтальных нагрузок. В данном исследовании рассматривается сейсмическая работа стен с раскосами из CFS, с особым вниманием к оптимизации стоечных элементов для их эффективной работы в качестве балок-колонн. В качестве исходного выбран и уточнён типичный поперечный профиль, основанный на коммерчески доступных сечениях, с целью максимизации несущей способности при соблюдении отраслевых стандартов и практических ограничений. Для двух рамных систем с раскосами разработаны модели методом конечных элементов (МКЭ), где выбранные сечения используются как для стоек, так и для хорд: одна рама использует коммерчески доступные профили CFS, а другая — оптимизированные сечения, ориентированные на повышение сейсмической устойчивости. В то время как традиционные конструкции учитывают действие вертикальных нагрузок, они часто игнорируют эффекты P-Δ; в данной работе эта проблема решается путём приложения различных уровней осевого сжатия для оценки влияния эффектов P-Δ на обе

разработанные модели. Несущая способность конструкций оценивается по соответствию критериям предельного дрейфа и предотвращению преждевременного разрушения, вызванного эффектами P-Δ в стоечных элементах хорд. Результаты дают ценные рекомендации по совершенствованию сейсмостойкого проектирования CFS-структур, предлагая систематическую стратегию оптимизации, улучшающую пластичность, надёжность и конструктивную целостность при сейсмических воздействиях.

Ключевые слова: холодногнутая сталь; стеновые панели с раскосами; оптимизация; вертикальная нагрузка; сейсмическая устойчивость.

References

1. M. Hasanali, K. Roy, S.M. Mojtabaei, I Hajirasouliha, GC Clifton, JBP Lim A critical review of cold-formed steel seismic resistant systems: Recent developments, challenges and future directions. Thin-Walled Structures 180, (2022) 109953.
2. D.T. Phan, S.M. Mojtabaei, I. Hajirasouliha, J. Ye, J.B.P Lim. Coupled Element and Structural Level Optimisation Framework for Cold-Formed Steel Frames, Journal of Constructional Steel Research, 49 (2019) 69-83.
3. Papargyriou, S.M. Mojtabaei, I. Hajirasouliha, J. Becque, K. Pilakoutas, Cold-formed steel beam-to- column bolted connections for seismic applications, Thin-Walled Structures, 172 (2022) 108876.
4. J. Ye, S.M. Mojtabaei, I. Hajirasouliha, K. Pilakoutas, Efficient design of cold-formed steel bolted-moment connections for earthquake resistant frames, Thin-Walled Structures, 59 (2019) 49-61.
5. J. Ye, S.M. Mojtabaei, I. Hajirasouliha. Seismic performance of cold-formed steel bolted moment connections with bolting friction-slip mechanism, Journal of Constructional Steel Research, 27 (2019) 86- 100.
6. S.M. Mojtabaei, I. Hajirasouliha, J. Ye, Optimisation of cold-formed steel beams for best seismic performance in bolted moment connections, Journal of Constructional Steel Research, 181 (2021) 106621.
7. S.M. Mojtabaei, M.Z. Kabir, I. Hajirasouliha, M. Kargar, Analytical and experimental study on the seismic performance of cold-formed steel frames. Journal of Constructional Steel Research 143, (2018) 18-31.
8. F. Yilmaz, S.M. Mojtabaei, I. Hajirasouliha, J. Becque, Behaviour and performance of OSB-sheathed cold- formed steel stud wall panels under combined vertical and seismic loading, Thin-Walled Structures, 183 (2023) 110419.
9. F. Yilmaz, J. Becque, S.M. Mojtabaei, I. Hajirasouliha, Capacity and Behavior of Sheathed Cold-Formed Steel Stud Walls under Outward Flexural Loading. Journal of Structural Engineering 151 (1), (2025) 04024192.
10. F. Yilmaz, J. Becque, S.M. Mojtabaei, I. Hajirasouliha, Experimental investigation of the behaviour and capacity of sheathed cold-formed steel stud walls under inward flexural loading. Thin-Walled Structures 192, (2024) 111048.
11. Al-Kharat, M.; Rogers, C.A. (2007) Inelastic performance of cold-formed steel strap braced walls. Journal of Constructional Steel Research 63, 4, p. 460–474.
12. Riahi, H.T. et al. (2020) Seismic collapse assessment of K-shaped bracings in cold-formed steel frames. Structures 27, p. 1803–1817.

13. Zeynalian, M.; Ronagh, H. (2013) Experimental study on seismic performance of strap-braced cold-formed steel shear walls. Advances in Structural Engineering 16, 2, p. 245–257.
14. Gad, E. et al. (1999) Lateral performance of cold-formed steel-framed domestic structures. Engineering Structures 21, 1, p. 83–95.
15. Rad, P.L. et al. (2024) Experimental investigation on seismic performance of cold-formed steel strap-braced stud walls under lateral cyclic and vertical loading. Thin-Walled Structures 194, p. 111312.
16. J. Ye, S.M. Mojtabaei, I. Hajirasouliha. Local-flexural interactive buckling of standard and optimised cold- formed steel columns, Journal of Constructional Steel Research, 144 (2018) 106-118.
17. J. Ye, S.M. Mojtabaei, I. Hajirasouliha, Paul Shepherd, Kypros Pilakoutas, Strength and deflection behaviour of cold-formed steel back-to-back channels. Engineering Structures 177 (2018) 641-654.
18. J. Ye, J. Becque, I. Hajirasouliha, S.M. Mojtabaei, J.B.P. Lim. Development of optimum cold-formed steel sections for maximum energy dissipation in uniaxial bending, Engineering Structures, 161 (2018) 55-67.
19. Mojtabaei, S.M. et al. (2021) Structural size optimization of single and built-up cold-formed steel beam-column members. Journal of Structural Engineering 147, 4, p. 04021030.
20. S.M. Mojtabaei, J. Ye, I. Hajirasouliha. Development of optimum cold-formed steel beams for serviceability and ultimate limit states using Big Bang-Big Crunch optimisation, Engineering Structures, 195 (2019) 172-181.
21. S.M. Mojtabaei, R. Khandan, I. Hajirasouliha, Predicting restraining effects in CFS channels: A machine learning approach, Steel and Composite Structures, An International Journal 51 (4), 441-456.
22. L. Simwanda, P. Gatheeshgar, F.M. Ilunga, B.D. Ikotun, S.M. Mojtabaei, Explainable machine learning models for predicting the ultimate bending capacity of slotted perforated cold-formed steel beams under distortional buckling, Thin-Walled Structures 205, (2024) 112587
23. S.M. Mojtabaei, J. Becque, I. Hajirasouliha, R. Khandan, Predicting the buckling behaviour of thin-walled structural elements using machine learning methods, Thin-Walled Structures, 184 (2023) 110518.
24. CEN (European Committee for Standardization) (2005) Eurocode 3: Design of steel structures – Part 1-1: General rules and rules for buildings. Brussels, Belgium.
25. CEN (European Committee for Standardization) (2005) Eurocode 3: Design of steel structures – Part 1-3: General rules – Supplementary rules for cold-formed members and sheeting. Brussels, Belgium.
26. Dassault Systèmes Simulia (2014) Abaqus 6.14 CAE User Guide.
27. D.T. Phan, S.M. Mojtabaei, I. Hajirasouliha, T. L. Lau, J.B.P Lim. Design and optimisation of cold-formed steel sections in bolted moment connections considering bimoment, Journal of Structural Engineering (ASCE), 146 (2020) 04020153.
28. S.M. Mojtabaei, J. Becque, I. Hajirasouliha. Local buckling in cold-formed steel moment resisting bolted connections: behaviour, capacity and design, Journal of Structural Engineering (ASCE), 146 (2020) 04020167
29. H. Parastesh, S.M. Mojtabaei, H. Taji, I. Hajirasouliha, A. Bagheri Sabbagh, Constrained optimization of anti-symmetric cold-formed steel beam-column sections, Engineering

Structures, 228 (2021) 111452.
30. S.M. Mojtabaei, J. Becque, I. Hajirasouliha, Behavior and Design of Cold-Formed Steel Bolted Connections Subjected to Combined Actions, Journal of Structural Engineering, 147 (2021) 04021013.
31. Pham, H.S.; Moen, C.D. (2015) *Stiffness and strength of single shear cold-formed steel screw-fastened connections.* Proceedings of the Annual Stability Conference, p. 1–12.
32. M. Hasanali, S.M. Mojtabaei, I. Hajirasouliha, G.C. Clifton, J.B.P. Lim, More accurate design equations for cold- formed steel members subjected to combined axial compressive load and bending, Thin-Walled Structures, 185 (2023) 110588.
33. M. Hasanali, S.M. Mojtabaei, G.C. Clifton, I. Hajirasouliha, S. Torabian, J.B.P. Lim, Capacity and design of cold- formed steel warping-restrained beam-column elements, Journal of Constructional Steel Research, 190 (2022) 107139.
34. F. Öztürk, S.M. Mojtabaei, M. Şentürk, S. Pul, I. Hajirasouliha, Buckling behaviour of cold-formed steel sigma and lipped channel beam–column members, Thin-Walled Structures, 173 (2022) 108963.
35. M. Hasanali, S.M. Mojtabaei, J.B.P. Lim, G.C. Clifton, I. Hajirasouliha, Optimized interaction equations for more efficient design of CFS channels under combined compression and biaxial bending. Journal of Structural Engineering 150 (8), (2024) 04024088.

Information about the authors

Muhammed Cosut -doctoral student of Sheffield university
Мухаммед Кошут - докторант (аспирант) Университета Шеффилда
Мухаммед Кошут -Шеффилд университетінің докторанты